20th Australasian Fluid Mechanics Conference
Perth, Australia
5-8 December 2016

An Immersed Boundary-Lattice Boltzmann Method for Swimming Sperms

F. B. Tian[1], J. Young[1] and J. C. S. Lai[1]

[1]School of Engineering and Information Technology, University of New South Wales, Canberra, ACT 2600, Australia

Abstract

This work presents an immersed boundary–lattice Boltzmann method for free-swimming sperms in an incompressible viscous fluid. This method involves sperm model, fluid solver and fluid–structure interaction (FSI). The sperm is simplified as a nonlinear beam. To drive the swimming motion, an internal moment is introduced into the beam equation. The fluid dynamics is obtained by solving the lattice Boltzmann equation. The FSI is handled by the immersed boundary method. Two numerical examples, one single sperm swimming in quiescent viscous fluid and two sperms in tandem arrangement, are presented to illustrate the efficiency of the present method.

Introduction

During their journey up the oviducts, only the few strongest sperms (out of hundreds of millions) will ever reach their destination. The winners have to swim in the right direction over distances that are around 1,000 times their own length in an extremely viscous fluid. During this journey, the sperms are exposed to different currents, and thus may utilise the hydrodynamic interaction benefit from other sperms around them or the oviduct walls so that they have a better chance to reach their destination. The underlying flow physics is complex and still has not been fully understood. Therefore, a numerical model for free-swimming sperms is a demanding task.

Among a variety of numerical methods (see Ref. [4] for a brief review), the immersed boundary method (IBM), first developed by Peskin [9], is extremely efficient for sperm swimming. An IBM was developed by Fauci and McDonald [6] to study the fluid dynamics of sperm motility near both rigid and elastic walls. Dillon et al. [5] developed a model to consider the motility of sperm flagella and cilia based on a common axonemal structure. More recently, Qin et al. [11] numerically studied the motion of a small swimmer in a viscous fluid by using the IBM. In their model, the force of the interaction between the swimmer and the fluid was calculated with a feedback law. With a prescribed traveling wave beating, the swimmer was propelled by the interaction force according to Newton's second law. Similar dynamic model has been extensively used for fish propulsion simulation [4, 13, 17, 21]. In the present work, we develop an immersed boundary–lattice Boltzmann method (IB-LBM) for free-swimming sperms in an incompressible viscous fluid.

Mathematical formulation and numerical method

Sperm dynamics

The geometrically nonlinear motion for the sperm is described as

$$K_v\frac{\partial \mathbf{X}}{\partial t}-\frac{\partial}{\partial s}\left[T(s)\frac{\partial \mathbf{X}}{\partial s}\right]+K_b\frac{\partial^4 \mathbf{X}}{\partial s^4}+\frac{\partial}{\partial s}\left(\frac{\partial M(s,t)}{\partial s}\mathbf{n}\right)=\mathbf{F}_f, \quad (1)$$

where s is the Lagrangian coordinate along the length from the leading edge to the tail, $T(s)=K_s(|\frac{\partial \mathbf{x}}{\partial s}|-1)$ is the tensile stress, K_s is the stretching coefficient, K_b is the bending rigidity, K_v is the viscous damping coefficient, $\mathbf{X}$ is the position vector of a point on the sperm, $\mathbf{n}$ is the normal vector, $M(s,t)$ is the internal driving moment, and $\mathbf{F}_f$ is the hydrodynamic stress exerted by the ambient fluid. The sperm is able to achieve different swimming gait by controlling M. Please note that we ignore the head of the sperm so that we can focus on the driving moment model.

Lattice Boltzmann method for incompressible viscous flow

The incompressible viscous fluid dynamics is approximately achieved by using the weak compressible LBM [1, 3]. In this method, the fluid kinematics is governed by the discrete lattice Boltzmann equation (LBE) of a single relaxation time model [1, 3, 14],

$$g_i(\mathbf{x}+\mathbf{e}_i\Delta t,t+\Delta t)-g_i(\mathbf{x},t)=-\frac{1}{\tau}[g_i(\mathbf{x},\mathbf{t})-g_i^{eq}(\mathbf{x},\mathbf{t})]+\Delta t G_i, \quad (2)$$

where $g_i(\mathbf{x},t)$ is the distribution function for particles with velocity $\mathbf{e}_i$ at position $\mathbf{x}$ and time t, Δt is the size of the time step, $g_i^{eq}(\mathbf{x},\mathbf{t})$ is the equilibrium distribution function, τ represents the nondimensional relaxation time, and G_i is the body-force term.

Here we use a two-dimensional nine-speed (D2Q9) model which has nine possible particle velocities,

$$\begin{aligned}
&\mathbf{e}_0=(0,0),\\
&\mathbf{e}_i=\left(\cos\frac{\pi(i-1)}{2},\sin\frac{\pi(i-1)}{2}\right)\frac{\Delta x}{\Delta t},\ (i=1-4),\\
&\mathbf{e}_i=\left(\cos\frac{\pi(i-9/2)}{2},\sin\frac{\pi(i-9/2)}{2}\right)\frac{\sqrt{2}\Delta x}{\Delta t},\ (i=5-8),
\end{aligned}$$

where Δx is the lattice spacing. In Eq. (2), g_i^{eq} and G_i are obtained by [7]

$$g_i^{eq}=\omega_i\rho\left[1+\frac{\mathbf{e}_i\cdot\mathbf{u}}{c_s^2}+\frac{\mathbf{uu}:(\mathbf{e}_i\mathbf{e}_i-c_s^2\mathbf{I})}{2c_s^4}\right], \quad (3)$$

$$G_i=\left(1-\frac{1}{2\tau}\right)\omega_i\left[\frac{\mathbf{e}_i-\mathbf{u}}{c_s^2}+\frac{\mathbf{e}_i\cdot\mathbf{u}}{c_s^4}\mathbf{e}_i\right]\cdot\mathbf{f}, \quad (4)$$

where ω_i are the weights given by $\omega_0=4/9$, $\omega_i=1/9$ for $i=1$ to 4 and $\omega_i=1/36$ for $i=5$ to 8, $\mathbf{u}=(u,v)$ is the velocity of the fluid, c_s is the speed of sound defined by $c_s=\Delta x/\sqrt{3}\Delta t$, and $\mathbf{f}$ is the body force acting on the fluid. The relaxation time is related to the kinematic viscosity in terms of

$$\nu=(\tau-0.5)c_s^2\Delta t. \quad (5)$$

Once the particle density distribution is known, the fluid density, velocity and pressure are then computed from

$$\rho=\sum_i g_i,\quad \mathbf{u}=(\sum_i \mathbf{e}_i g_i+0.5\mathbf{f}\Delta t)/\rho,\quad p=\rho c_s^2. \quad (6)$$

Immersed boundary method

The immersed boundary method [10] is extended to handle the moving boundary. In this method, the boundary condition is taken into account by spreading the surface force onto the volumetric fluid grids in the vicinity of the boundary and treating it as a body force, according to,

$$\mathbf{f}(\mathbf{x},t)=\int \mathbf{F}(s,t)\delta_D(\mathbf{x}-\mathbf{X}(\mathbf{s},t))d\mathbf{s}, \quad (7)$$

where $\mathbf{F}(s,t)$ is the Lagrangian force density on the fluid by the elastic boundary, $\delta_D(\mathbf{x}-\mathbf{X}(\mathbf{s},t))$ is Dirac's delta function. Since $\mathbf{F}(s,t)$ is the reaction force of $\mathbf{F}_f$ in Eq. (1), it can be written as

$$\mathbf{F}(s,t) = -\mathbf{F}_f = \mathbf{F}_v(s,t) + \mathbf{F}_s(s,t) + \mathbf{F}_b(s,t) + \mathbf{F}_d(s,t), \qquad (8)$$

where $\mathbf{F}_v$, $\mathbf{F}_s$, $\mathbf{F}_b$ and $\mathbf{F}_d$ are respectively the viscous, stretching, bending, and internal driving forces, and are given by

$$\mathbf{F}_v(s,t) = -K_v \frac{\partial \mathbf{X}}{\partial t}, \;\; \mathbf{F}_s(s,t) = \frac{\partial}{\partial s}\left[T(s)\frac{\partial \mathbf{X}}{\partial s}\right],$$
$$\mathbf{F}_b(s,t) = -K_b \frac{\partial^4 \mathbf{X}}{\partial s^4}, \;\; \mathbf{F}_d(s,t) = -\frac{\partial}{\partial s}\left(\frac{\partial M(s,t)}{\partial s}\mathbf{n}\right).$$

The velocity of the sperm is interpolated from the flow field, and the position of the sperm is updated explicitly, i.e.,

$$\mathbf{U}(s,t) = \int \mathbf{u}(\mathbf{x},t)\delta_D(\mathbf{x}-\mathbf{X}(s,t))d\mathbf{x}, \qquad (9)$$

$$\frac{\partial \mathbf{X}(s,t)}{\partial t} = \mathbf{U}(s,t), \qquad (10)$$

where $\mathbf{U}(s,t)$ is the velocity of the sperm.

A 2^{nd}-order finite-difference scheme is used to compute $\mathbf{F}_s$, $\mathbf{F}_b$ and $\mathbf{F}_d$. The time integration of Eq. (10) is conduced according to

$$\mathbf{X}^{n+1} = \mathbf{X}^n + \Delta t \mathbf{U}^{n+1}. \qquad (11)$$

The immersed boundary-lattice Boltzmann method in this work has been validated and verified in our previous studies (see e.g. Refs. [14, 19]), and has been used to study filament(s) flapping in viscous fluids [12, 15, 16] and cell/particle flows [18, 20]. In the present work we do not repeat the validations, as the driving moment and viscous force are introduced into the structure dynamics without introducing new numerical difficulties.

Numerical examples

A Single sperm swimming forward

We first consider a single sperm swimming forward in an incompressible viscous fluid. The driving moment is given as a traveling wave, $M = A\sin(2\pi(s-ct)/\lambda)$, where A is the amplitude, λ is the wavelength, and c is the phase speed. The length of the sperm at maximum extension is L. The fluid density ρ, phase speed c and sperm length L are used as the reference quantities, and the governing non-dimensional parameters are: $Re = \rho cL/\mu = 2$, $A/(\rho c^2 L^2) = 0.4$, $L/\lambda = 2$, $K_b/(\rho c^2 L^3) = 0.02$, $K_s/(\rho c^2 L) = 3200$, and $K_v/(\rho c) = 0$. The computational domain is a $40L \times 20L$ rectangular box discretized by 2001×1001 uniform Cartesian nodes. The sperm is initially located at $(35L, 10L)$ at steady state and approaches to a virtual target at $(0, 10L)$. In order to maintain its swimming direction, a control moment is applied if its direction is not the same as that pointing from its position to the target.

Figure 1 shows the sperm profiles during start and steady swimming stages. From Fig. 1(a) it is found that a traveling wave will be generated when a moment traveling wave is applied, and thus, a forward swimming motion will be driven. After an accelerating stage, the sperm performs steady swimming as shown in Fig. 1(b).

The leading edge trajectory, and speeds in x- and y-directions are shown in Fig. 2. It shows that the swimming path is an up-and-down wave which is due to the sinusoidal driving moment.

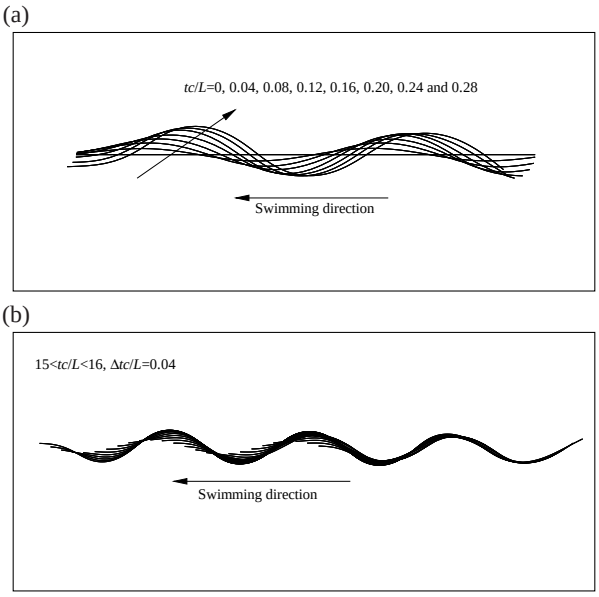

Figure 1: (a) Start stage and (b) steady swimming stage.

The sperm does not directly swim to the target point. Instead, the swimming direction biases to left first, and then is adjusted to right. Finally, the sperm swims directly at the target. The deviation during the start is due to the asymmetric moment. A continuous control moment is applied to adjust the swimming direction. This start-adjustment stage happens in the first 9 or 10 cycles, as shown in Fig. 2(b). Furthermore, the average forward swimming speed is close to 0.95. This number is different from other simulations [13] in fish swimming. This is caused by the control moment which also contributes energy to propel the sperm. In addition, the lateral swimming amplitude is 0.3, and is much larger compared to that observed for fish swimming [2]. This is due to the low Reynolds number or high viscous force in the present application.

Figure 3 shows the instantaneous vorticity and pressure contours at tL/c=15.0. It is found that there is no vortex street in the wake. This observation is different from the traveling wave propulsion of fish [4], but similar to the traveling surface propulsion [13]. Ref. [13] also reported a backward jet outside the shear layer near the traveling surface. However, we do not observe such a jet for the sperm swimming due to the highly viscous fluid in this application. Therefore, the thrust is generated by the high pressure on the leeward side and low pressure on the upwind side, as demonstrated in Fig. 3(b).

Two sperms in tandem arrangement

As a second application, two sperms initially located in tandem, are considered. The initial locations of the sperms are $(35L, 10L)$ and $(33.2L, 10L)$, respectively, with initial separation between two sperm being $0.8L$.

Figure 4 shows the sperm profiles during start, unstable and regulating stages. It is found that there is no significant difference between single sperm and two sperms in tandem arrangement at the start stage. However, the two-sperm system loses its stability when two sperms are close enough, and both deviate from the correct direction at a distance $x/L = 15$ from the target point, which is due to the high pressure near the head of the trailing sperm. When the sperms detect the deviations, the control moment is activated to adjust the forward swimming direction. This adjustment process can be demonstrated by profiles shown

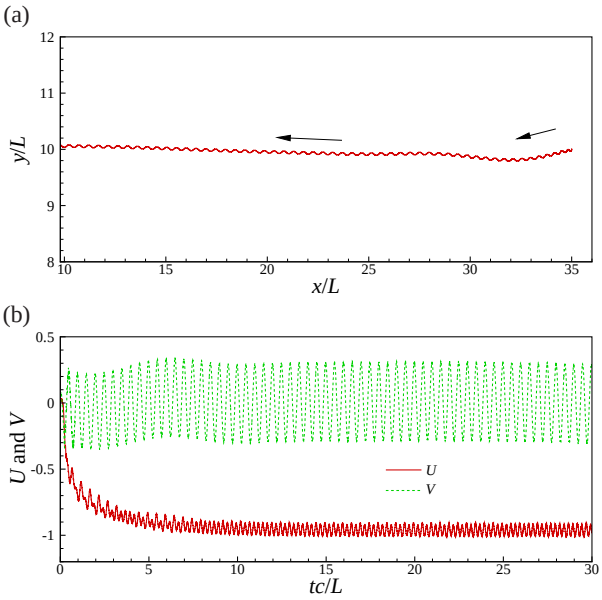

Figure 2: (a) Leading edge trajectory and (b) speeds in x- and y-directions.

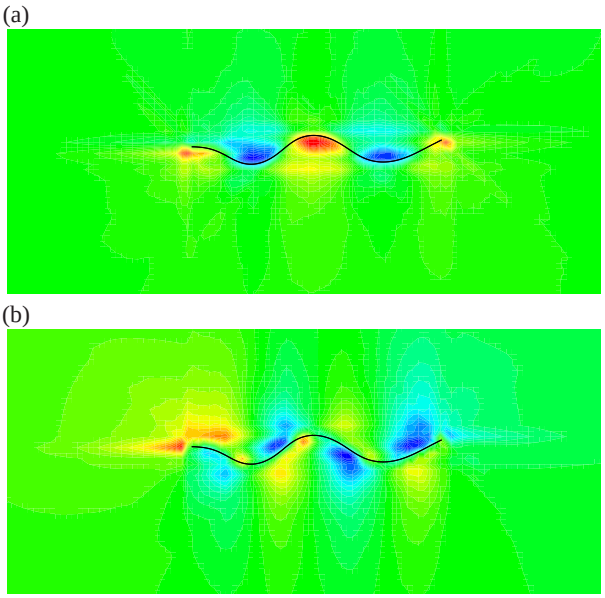

Figure 3: (a) Vorticity contours and (b) pressure contours at tL/c=15.0.

in Fig. 4(c).

The leading edge trajectories, and x- and y-direction speeds of the sperms are shown in Fig. 5. At the starting stage, similar swimming deviation is observed, and soon the swimming is tuned to the right direction. We also note that the acceleration of the two-sperm system is larger than the single sperm, and that the forward speed of the two-sperm system is larger. Therefore, the two sperms enjoy benefits from the interaction in terms of acceleration and forward speed. During the unstable and regulating stages, the speed of the trailing sperm is larger compared to that of the leading one, and soon the trailing one catches up to the leading one, as shown in Fig. 5(a). If larger computational domain and longer time are applied, the process that the leading one catches up to the trailing one can be captured. These phenomena imply that there are both collaboration and competition between two sperms [8].

Figure 6 shows the instantaneous vorticity contours at $tc/L = 15.0$ when the instability occurs. The major difference compared to the single sperm case is the asymmetrical structure of the leading sperm with respect to its mid-perpendicular. This phenomenon is caused by the pressure-induced instability, and further disturbs the swimming gait.

Conclusion

A numerical approach combining the immersed boundary method and the lattice Boltzmann method is introduced to simulate fluid–structure interaction (FSI) of free-swimming sperms in a highly viscous fluid. This method is composed of three parts: a sperm model simplified as a nonlinear beam, fluid solver using the lattice Boltzmann method, and FSI achieved by the immersed boundary method. Two numerical examples are conducted to illustrate the effectiveness of the present method. The first case is a single sperm swimming in a quiescent fluid. The numerical results show that both driving and controlling moments work properly to drive the swimming motion and to control the swimming direction, respectively. The other case is two sperms initially located in tandem. It is found that the two sperms enjoy benefits from the interaction in terms of acceleration and forward speed. In addition, the trailing sperm catches up to the leading one after an unstable-adjusting process implying that there is both collaboration and competition between two sperms.

Acknowledgements

Dr. F.-B. Tian is the recipient of an Australian Research Council Discovery Early Career Researcher Award (project number DE160101098). This work was partly supported by the Rector's Start-Up grant, UNSW Canberra, and was partly undertaken on the NCI National Facility in Canberra, Australia, which is supported by the Australian Commonwealth Government.

References

[1] Aidun, C. K. and Clausen, J. R., Lattice-Boltzmann method for complex flows, *Annu. Rev. Fluid Mech.*, **42**, 2010, 439–472.

[2] Carling, J., Williams, T. L. and Bowtell, G., Self-propelled anguilliform swimming: simultaneous solution of the two-dimensional Navier–Stokes equations and Newton's laws of motion, *J. Exp. Biol.*, **201**, 1998, 3143–3166.

[3] Chen, S. and Doolen, G. D., Lattice Boltzmann method for fluid flows, *Annu. Rev. Fluid Mech.*, **30**, 1998, 329–364.

[4] Deng, H. B., Xu, Y. Q., Chen, D. D., Dai, H., Wu, J. and Tian, F. B., On numerical modeling of animal swimming and flight, *Comput. Mech.*, **52**, 2013, 1221–1242.

[5] Dillon, R. H., Fauci, L. J. and Yang, X., Sperm motility and multiciliary beating: an integrative mechanical model, *Comput. Math. Appl.*, **52**, 2006, 749–758.

[6] Fauci, L. J. and McDonald, A., Sperm motility in the presence of boundaries, *Bulletin of Mathematical Biology*, **57**, 1995, 679–699.

[7] Guo, Z. L., Zheng, C. G. and Shi, B. C., Discrete lattice effects on the forcing term in the lattice Boltzmann method, *Phys. Rev. E*, **65**, 2002, 046308.

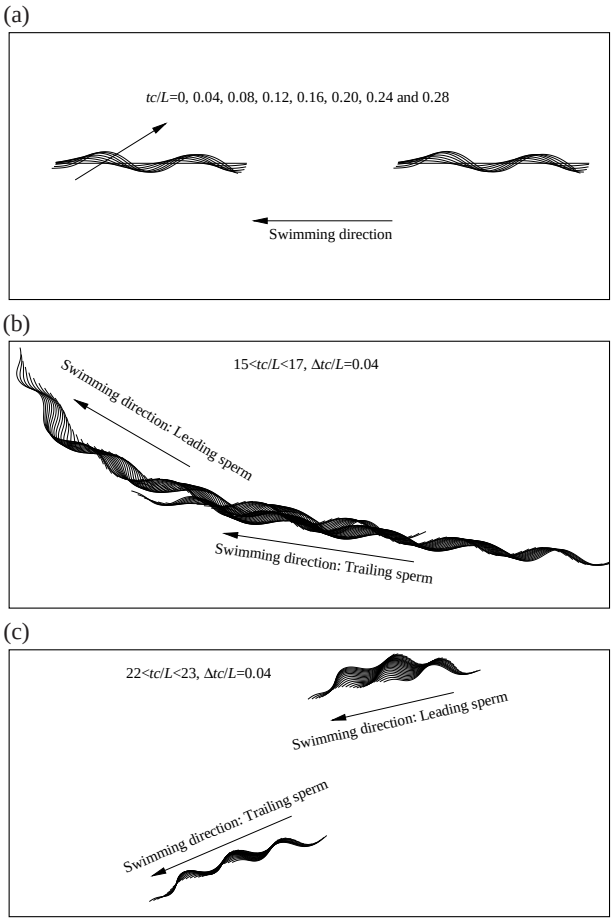

Figure 4: Sperm profiles during (a) start stage, (b) unstable stage and (c) regulating stage.

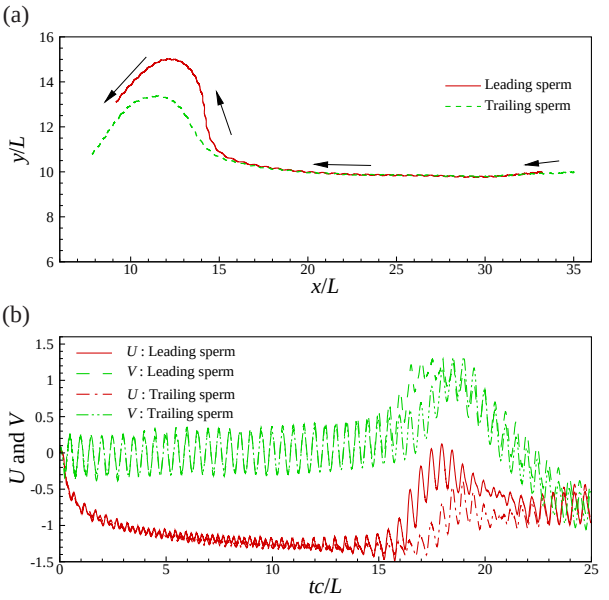

Figure 5: (a) Leading edge trajectories and (b) speeds in x- and y-direction.

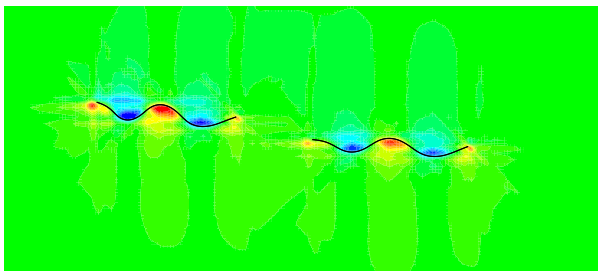

Figure 6: Instantaneous vorticity contours at $tc/L = 15.0$.

[8] Koch, D. L. and Subramanian, G., Collective hydrodynamics of swimming microorganisms: living fluids, *Annu. Rev. Fluid Mech.*, **43**, 2011, 637–659.

[9] Peskin, C. S., *Flow patterns around heart valves: a digital computer method for solving the equations of motion*, Ph.D. thesis, Yeshiva University, 1972.

[10] Peskin, C. S., Flow patterns around heart valves: A numerical method, *J. Comput. Phys.*, **10**, 1972, 252–271.

[11] Qin, F. H., Huang, W. X. and Sung, H. J., Simulation of small swimmer motions driven by tail/flagellum beating, *Compt. Fluids*, **55**, 2012, 109–117.

[12] Tian, F. B., Role of mass on the stability of flag/flags in uniform flow, *Appl. Phys. Lett.*, **103**, 2013, 034101.

[13] Tian, F. B., Lu, X. Y. and Luo, H., Propulsive performance of a body with a traveling wave surface, *Phys. Rev. E*, **86**, 2012, 016304.

[14] Tian, F. B., Luo, H., Zhu, L., Liao, J. C. and Lu, X. Y., An immersed boundary-lattice Boltzmann method for elastic boundaries with mass, *J. Comput. Phys.*, **230**, 2011, 7266–7283.

[15] Tian, F. B., Luo, H., Zhu, L. and Lu, X. Y., Interaction between a flexible filament and a downstream rigid body, *Phys. Rev. E*, **82**, 2010, 026301.

[16] Tian, F. B., Luo, H., Zhu, L. and Lu, X. Y., Coupling modes of three filaments in side-by-side arrangement, *Phys. Fluids*, **23**, 2011, 111903.

[17] Tian, F. B., Xu, Y. Q., Tang, X. Y. and Deng, Y. L., Study on a self-propelled fish swimming in viscous fluid by a finite element method, *J. Mech. Med. Biol.*, **13**, 2013, 1340012.

[18] Xu, Y. Q., Tang, X. Y., Tian, F. B., Peng, Y. H., Xu, Y. and Zeng, Y. J., IB–LBM simulation of the hemocyte dynamics in a stenotic capillary, *Comput. Method Biomec.*, **17**, 2014, 978–985.

[19] Xu, Y. Q., Tian, F. B. and Deng, Y. L., An efficient red blood cell model in the frame of IB–LBM and its application, *Int. J. Biomath.*, **6**, 2013, 1250061.

[20] Xu, Y. Q., Tian, F. B., Li, H. J. and Deng, Y. L., Red blood cell partitioning and blood flux redistribution in microvascular bifurcation, *Theor. Appl. Mech. Lett.*, **2**, 2012, 024001.

[21] Yeo, K. S., Ang, S. J. and Shu, C., Simulation of fish swimming and manoeuvring by an SVD–GFD method on a hybrid meshfree–Cartesian grid, *Comput. Fluids*, **39**, 2010, 403–430.